Int. J. Heat Mass Transfer. Vol. 35, No. 8, pp. 2043–2052, 1992
Printed in Great Britain

0017–9310/92 $5.00 + 0.00
Pergamon Press Ltd

The boundary condition of the P_N-approximation used to solve the radiative transfer equation

FENGSHAN LIU
Department of Fuel and Energy, University of Leeds, Leeds LS2 9JT, U.K.

and

JIM SWITHENBANK and ERIC S. GARBETT
Department of Mechanical and Process Engineering, University of Sheffield, Sheffield S1 3JD, U.K.

(*Received* 22 *February* 1991 *and in final form* 9 *August* 1991)

Abstract—The arbitrariness of the boundary condition applied to the P_1-approximation is explored by extending the conventional Marshak boundary condition to include an arbitrary constant. The influence of the constant on the results of the P_1-approximation is investigated numerically for one- and multi-dimensional radiative heat transfer problems. Based on these numerical investigations, optimized values for the constant are recommended according to the wall emissivity of the radiating system. The accuracy of the P_1-approximation can be improved significantly when optimized values are employed in the boundary condition.

1. INTRODUCTION

RADIATIVE heat transfer is the predominant energy transfer mode in most industrial combustion systems because such systems usually involve high temperatures and large geometrical dimensions. Unfortunately, radiative heat transfer is governed by a complex integro-differential equation in the radiation intensity which is extremely difficult to solve even for one-dimensional problems. Exact solutions to the radiative transfer equation exist only for some limited situations [1]; hence, approximate solution methods are of interest for the purpose of modelling radiative heat transfer in practical combustion systems. Over the years, several numerical methods have been developed to solve the radiative transfer equation, such as the zone method, the Monte Carlo method, flux models and the discrete transfer method. However, each method suffers from some shortcomings which restrict its use. Comprehensive discussions of these methods have been presented (see ref. [1], for example); therefore, it is not necessary to repeat them here.

Recently, lower order spherical harmonics methods, such as the P_1- and the P_3-approximations, have received considerable research attention on account of their simplicity, compatibility with the finite difference modelling technique and capability of handling anisotropic scattering [2, 3]. However, the P_N-approximation method suffers from the boundary condition ambiguity which has not been widely studied, although attention has been drawn to it in the literature [3–5].

Two different schemes of boundary condition approximation have been developed for application to the spherical harmonics method in the work related to neutron transport theory, named Mark's and Marshak's boundary conditions [4, 6]. It has been pointed out that Mark's boundary condition is preferable for high order approximations ($N > 3$); however, Marshak's boundary condition gives better results for lower order approximations, such as the P_1- and the P_3-approximations [4]. Therefore, Marshak's boundary condition has been widely used in the literature. The pronounced shortcoming of the P_1- and P_3-approximations when employing Marshak's boundary condition, as addressed by Ratzel and Howell [7], is to overpredict the surface heat transfer characteristics.

The objective of this work is to improve the accuracy of the P_N-approximation by investigating its boundary conditions. In order to simplify the discussion, this paper focuses on the boundary condition of the P_1-approximation. However, it should be pointed out that the underlying ideas are also applicable to the P_3-approximation. In the next section, the formulation of the P_1-approximation is given without derivation. The arbitrariness of the boundary condition of the P_1-approximation is demonstrated by formulating a more general form of boundary condition which contains an arbitrary constant. By studying the effect of the value of the constant on the result of the P_1-approximation, optimized values of the constant are recommended. It is shown in this work

NOMENCLATURE

$E_3(x)$	third exponential integral
I	radiation intensity [$W m^{-2} sr^{-1}$]
I_0	zero moment of radiation intensity [$W m^{-2}$]
I_i	first order moment of radiation intensity [$W m^{-2}$]
I_b	black-body radiation intensity [$W m^{-2} sr^{-1}$]
l_i	direction cosines: ξ if $i = 1$; η if $i = 2$; μ if $i = 3$
L	distance between two parallel plates
q	net radiative heat flux [$W m^{-2}$]
q^+	component of radiative heat flux in the positive direction
q^-	component of radiative heat flux in the negative direction
Q	non-dimensional net radiative heat flux
S	volumetric heat generation rate [$kW m^{-3}$]
T	temperature [K]
x, y, z	Cartesian coordinates [m].

Greek symbols

ε	emissivity
θ	polar angle [sr]; non-dimensional black-body radiation intensity
κ_α	absorption coefficient [m^{-1}]
ξ, η, μ	direction cosines
τ_0	optical dimension
ϕ	azimuthal angle [sr]
Ω	solid angle [sr].

Subscripts

e	exact solution
g	gas
w	wall.

that the accuracy of the P_1-approximation can be improved significantly when the optimized values are employed.

2. FORMULATION

2.1. *Governing equation of the P_1-approximation*

For an absorbing–emitting medium, under the assumptions that the medium is grey and in local thermodynamic equilibrium, the time-independent radiative transfer equation in a three-dimensional Cartesian coordinate system is given by

$$\frac{\partial I}{\partial x}\xi+\frac{\partial I}{\partial y}\eta+\frac{\partial I}{\partial z}\mu=-\kappa_\alpha I+\kappa_\alpha I_b(T) \quad (1)$$

where ξ, η and μ are direction cosines defined as

$$\xi=\sin\theta\cos\phi,\quad \eta=\sin\theta\sin\phi,\quad \mu=\cos\theta. \quad (2)$$

In the P_1-approximation, the radiation intensity is expanded in terms of its moments as

$$I(x,y,z,\theta,\phi)=\frac{1}{4\pi}[I_0+3(I_1\xi+I_2\eta+I_3\mu)] \quad (3)$$

where I_0 and I_i $(i = 1, 2, 3)$ are the zero order moment and the first order moments of the intensity defined as

$$I_0(x,y,z)=\int_0^{2\pi}\int_0^{\pi} I(x,y,z,\theta,\phi)\sin\theta\,d\theta\,d\phi \quad (4)$$

$$I_i(x,y,z)=\int_0^{2\pi}\int_0^{\pi} l_i I(x,y,z,\theta,\phi)\sin\theta\,d\theta\,d\phi \quad (5)$$

where l_i is either ξ, η or μ depending on i. For example, if $i = 1$, $l_i = \xi$. Note that the first order moments, I_i, are the net radiative heat fluxes. After performing some standard derivations (see Menguc and Viskanta [2]), the governing equation of the P_1-approximation can be obtained as

$$\frac{\partial^2 I_0}{\partial x^2}+\frac{\partial^2 I_0}{\partial y^2}+\frac{\partial^2 I_0}{\partial z^2}=3\kappa_\alpha^2(I_0-4\pi I_b). \quad (6)$$

If the volumetric heat generation rate S of the medium is specified, the governing equation of the P_1-approximation then takes the form

$$\frac{\partial^2 I_0}{\partial x^2}+\frac{\partial^2 I_0}{\partial y^2}+\frac{\partial^2 I_0}{\partial z^2}=3\kappa_\alpha S. \quad (7)$$

The net radiative heat fluxes, I_i, are related to I_0 through

$$I_1=-\frac{1}{3\kappa_\alpha}\frac{\partial I_0}{\partial x} \quad (8)$$

$$I_2=-\frac{1}{3\kappa_\alpha}\frac{\partial I_0}{\partial y} \quad (9)$$

$$I_3=-\frac{1}{3\kappa_\alpha}\frac{\partial I_0}{\partial z}. \quad (10)$$

The net radiative heat flux, q_i, can also be written as the difference between the forward and backward components such that

$$q_i=q_i^+-q_i^-. \quad (11)$$

In the P_1-approximation, q_i^+ and q_i^- are expressed as

$$q_i^+=\tfrac{1}{4}I_0+\tfrac{1}{2}I_i \quad (12)$$

$$q_i^-=\tfrac{1}{4}I_0-\tfrac{1}{2}I_i. \quad (13)$$

2.2. *Marshak's boundary condition*

In most practical combustion systems, the wall surfaces can be assumed to be diffusively reflecting and emitting. This means that the outgoing radiation intensity at the boundary is isotropic, i.e. independent of direction. The outgoing radiation intensity at such a surface is obtained by considering radiative energy conservation and can be written as

$$I_w = \varepsilon_w I_b(T_w) + (1-\varepsilon_w)\frac{1}{\pi}\int_{\Omega=2\pi} l_i I \, d\Omega. \quad (14)$$

The exact boundary condition is expressed as

$$I = I_w. \quad (15)$$

Equation (14) is effectively equivalent to

$$q_i^{\pm} = \varepsilon_w \pi I_b(T_w) + (1-\varepsilon_w) q_i^{\mp} \quad (16)$$

where $\pm$ corresponds to the surfaces at the positive and negative directions, respectively. It should be pointed out that substitution of the radiation intensity distribution, equation (3), into the exact boundary condition, equation (15), does not yield an applicable boundary condition for the P_1-approximation since the angular dependence of intensity still remains in the expression. Marshak's boundary condition for the P_1-approximation is obtained by taking the integral of the radiation intensity over the appropriate hemisphere after first multiplying by the appropriate direction cosine such that

$$\int_{\Omega=2\pi} I l_i \, d\Omega = \int_{\Omega=2\pi} I_w l_i \, d\Omega. \quad (17)$$

Substitution of equations (3) and (14) into equation (17) leads to

$$I_0 \pm \frac{2(2-\varepsilon_w)}{\varepsilon_w} I_i = 4\pi I_b(T_w). \quad (18)$$

In fact, Marshak's boundary condition, equation (18), can also be obtained by substituting equations (12) and (13) into equation (16). Therefore, Marshak's boundary condition ensures the conservation of radiative energy at boundaries. Note that I_i are related to I_0 through equations (8)–(10).

2.3. *Extensions of Marshak's boundary condition*

Two schemes for modifying Marshak's boundary condition are presented in this section. The starting point of the first scheme is the realization that the procedure of achieving the boundary condition for the P_1-approximation suffers from a certain ambiguity, although it has not been addressed explicitly.

In applying any of the P_N-approximation methods, we encounter the difficulty that the radiation intensity is represented by a truncated spherical harmonics series, so that the correct boundary condition of equation (15) cannot be satisfied exactly. This can be well understood since the governing equations of the P_N-approximation require relations between the moments of the intensity and the wall temperature as boundary conditions; however, the exact boundary condition is given for the intensity itself. As a result, the exact boundary condition, equation (15), cannot be used directly as the working boundary condition for the P_N-approximation as mentioned above. Therefore, it has to be concluded that any usable boundary conditions for the P_N-approximation are exact only in an integral sense. The first scheme for extending Marshak's boundary condition is to replace equation (17) by a general integral form of the exact boundary condition such that

$$\int_{\Omega=2\pi} I f(\Omega) \, d\Omega = \int_{\Omega=2\pi} I_w f(\Omega) \, d\Omega \quad (19)$$

where $f(\Omega)$ is an arbitrary function of direction. It is clear that equation (19) involves a certain arbitrariness due to the introduction of the arbitrary function. In order to obtain an analytical expression for equation (19), it is assumed in this work that $f(\Omega)$ has the form

$$f(\Omega) \propto l_i^n \quad (20)$$

where n is an arbitrary positive integer or zero. Then the more general form of boundary condition for the P_1-approximation will be derived from equation (21)

$$\int_{\Omega=2\pi} I l_i^n \, d\Omega = \int_{\Omega=2\pi} I_w l_i^n \, d\Omega. \quad (21)$$

Equation (21) has physical significance for $n = 0$, 1 and 2. $n = 0$, 1 and 2 correspond, respectively, to the conditions that the radiation energy density, radiative energy and radiation stress are exact at the boundary considered. It is worth mentioning that equation (19) or equation (21) can be readily applied to the P_3-approximation. Substitution of equations (3) and (14) into equation (21) yields

$$I_0 \pm \frac{3k+2(1-\varepsilon_w)}{\varepsilon_w} I_i = 4\pi I_b(T_w) \quad (22)$$

where k is a constant given as

$$k = \frac{\int_{\Omega=2\pi} l_i^{n+1} \, d\Omega}{\int_{\Omega=2\pi} l_i^n \, d\Omega}. \quad (23)$$

Employing the recurrence relation between $\int_{\Omega=2\pi} l_i^{n+1} \, d\Omega$ and $\int_{\Omega=2\pi} l_i^n \, d\Omega$ [8], it turns out that k is simply evaluated as

$$k = \frac{n+1}{n+2}. \quad (24)$$

Note that the boundary condition of equation (22) automatically includes the widely used Marshak boundary condition when n takes the value of 1. It is also noteworthy that equation (22) can be rewritten as

$$\frac{1}{4}I_0 \pm \frac{3k}{4}I_i = \varepsilon_w \pi I_b(T_w) + (1-\varepsilon_w)(\tfrac{1}{4}I_0 \mp \tfrac{1}{2}I_i). \quad (25)$$

By comparing equation (25) with equation (16), it can be seen that at boundaries having a positive normal direction

$$q_i^+ = \tfrac{1}{4}I_0 + \tfrac{3}{4}kI_i \quad (26)$$

$$q_i^- = \tfrac{1}{4}I_0 - \tfrac{1}{2}I_i \quad (27)$$

while at boundaries having a negative direction

$$q_i^+ = \tfrac{1}{4}I_0 + \tfrac{1}{2}I_i \quad (28)$$

$$q_i^- = \tfrac{1}{4}I_0 - \tfrac{3}{4}kI_i. \quad (29)$$

These equations demonstrate that radiative energy is not conserved at boundaries if n is not equal to 1. This is not surprising because the condition imposed on the radiation intensity by equation (21) is less strict than that by equation (15).

The second scheme to modify Marshak's boundary condition is to extend the suggestion of Pomraning and Foglesong [5]. Instead of using equations (12) and (13), they suggest expressing the forward and backward components of radiative heat flux at boundaries as

$$q_i^+ = \tfrac{1}{4}I_0 + (1-\delta)I_i \quad (30)$$

$$q_i^- = \tfrac{1}{4}I_0 - \delta I_i \quad (31)$$

where δ is an arbitrary constant. Note that equations (30) and (31) ensure the conservation of radiative energy at boundaries. Substitution of equations (30) and (31) into equation (16) yields the other modified boundary condition for the P_1-approximation

$$I_0 \pm \frac{4-4\varepsilon_w\delta}{\varepsilon_w} I_i = 4\pi I_b(T_w). \quad (32)$$

This generalized boundary also includes Marshak's boundary condition when δ is equal to 0.5. It should be pointed out that this scheme of modification cannot be easily applied to the P_3-approximation. Moreover, it can be expected that the variation of δ will affect the solution of the P_1-approximation in a similar way as that caused by altering the value of n. Therefore, the relation between I_0 and I_i at boundaries given in equation (32) will not be used as the boundary condition to obtain the solution of the P_1-approximation in this work.

The effects of n on the P_1-approximation solution will be shown in the next section for some one- and multi-dimensional problems by comparing the numerical results of the P_1-approximation with exact solutions.

3. RESULTS

Numerical results of the P_1-approximation reported in this paper for multi-dimensional problems were obtained by using the elliptic equation successive-overrelaxation (SOR) iterative technique. All results to be shown were computed on the PRIME computer at the University of Sheffield, U.K. Results for a one-dimensional case were calculated based on its analytical solution. The accuracy of the numerical scheme for multi-dimensional problems was assessed by comparing the results of the P_1-approximation obtained in this work with those available in the literature [7, 9]. For all cases examined, the numerical results of this work are exactly the same as published data when Marshak's boundary condition is used.

3.1. *One-dimensional planar media*

Consider the radiative heat transfer between two parallel, infinite, diffuse surfaces bounding an isothermal, homogeneous, absorbing and emitting medium (Fig. 1). The direction perpendicular to the surfaces is chosen as the reference direction. The two walls have different temperatures, T_{w1} and T_{w2}, but have the same emissivity, ε_w. For this problem the exact solution of the non-dimensional radiative heat transfer rate, non-dimensionalized by $\pi I_b(T_g)$, to Wall 1 (see Fig. 1) can be readily written as [10]

$$Q_e(0) = 2C_2E_3(\tau_0) - C_1 \quad (33)$$

where

$$C_1 = \frac{\varepsilon_w\theta_1 + [2\varepsilon_w(1-\varepsilon_w)E_3(\tau_0)]\theta_2 - [\varepsilon_w + 2\varepsilon_w(1-\varepsilon_w)E_3(\tau_0)]}{1-(1-\varepsilon_w)^2[2E_3(\tau_0)]^2} \quad (34)$$

$$C_2 = \frac{\varepsilon_w\theta_2 + [2\varepsilon_w(1-\varepsilon_w)E_3(\tau_0)]\theta_1 - [\varepsilon_w + 2\varepsilon_w(1-\varepsilon_w)E_3(\tau_0)]}{1-(1-\varepsilon_w)^2[2E_3(\tau_0)]^2} \quad (35)$$

$$\theta_1 = \frac{I_b(T_{w1})}{I_b(T_g)} \quad (36)$$

$$\theta_2 = \frac{I_b(T_{w2})}{I_b(T_g)} \quad (37)$$

$$\tau_0 = \kappa_a L \quad (38)$$

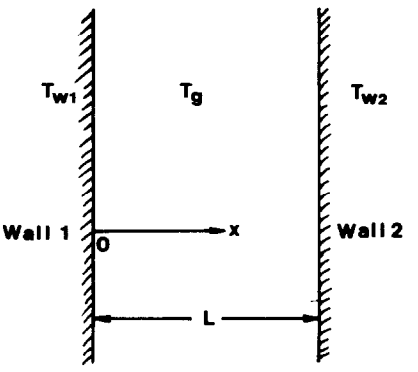

FIG. 1. Parallel walls separated by an absorbing–emitting medium.

$$E_3(x) = \int_0^1 \exp(-x/t)t\,dt. \tag{39}$$

$E_3(x)$ is the third exponential integral. Tabulation of $E_3(x)$ can be found in the book by Siegel and Howell [11].

In the P_1-approximation, the heat transfer rate to Wall 1 is evaluated as

$$q(0) = \frac{1}{3\kappa_\alpha}\frac{dI_0}{dx}\bigg|_{x=0}. \tag{40}$$

I_0 can be written analytically under the physical conditions given in Fig. 1, using the boundary condition of equation (22), such that

$$I_0 = 4\pi I_b(T_g) + \pi I_b(T_g)(a_1 \exp(\sqrt{3}\kappa_\alpha x) + a_2 \exp(-\sqrt{3}\kappa_\alpha x)) \tag{41}$$

where

$$a_1 = \frac{4\left[(\theta_2-1)\left(1+\frac{\sqrt{3}}{3}r\right)\exp(-\sqrt{3}\tau_0) - (\theta_1-1)\left(1-\frac{\sqrt{3}}{3}r\right)\exp(-2\sqrt{3}\tau_0)\right]}{\left(1+\frac{\sqrt{3}}{3}r\right)^2 - \left(1-\frac{\sqrt{3}}{3}r\right)^2\exp(-2\sqrt{3}\tau_0)} \tag{42}$$

$$a_2 = \frac{4\left[(\theta_1-1)\left(1+\frac{\sqrt{3}}{3}r\right) - (\theta_2-1)\left(1-\frac{\sqrt{3}}{3}r\right)\exp(-\sqrt{3}\tau_0)\right]}{\left(1+\frac{\sqrt{3}}{3}r\right)^2 - \left(1-\frac{\sqrt{3}}{3}r\right)^2\exp(-2\sqrt{3}\tau_0)} \tag{43}$$

$$r = \frac{3k+2(1-\varepsilon_w)}{\varepsilon_w}. \tag{44}$$

Then the non-dimensional heat transfer rate to Wall 1, $Q(0)$, can be calculated as

$$Q(0) = \frac{q(0)}{\pi I_b(T_g)} = \frac{\sqrt{3}}{3}(a_1 - a_2). \tag{45}$$

For given wall temperatures, wall emissivities and medium temperature, the radiative heat transfer rate to Wall 1 is a function of the optical dimension τ_0. It is of interest to compare the heat transfer rates to Wall 1 predicted by the P_1-approximation with the exact solutions when the optical dimension τ_0 tends to zero and infinity.

Consider first the limit of $\tau_0 \to 0$. The exact solution of equation (33) yields

$$\lim_{\tau_0\to 0} Q_e(0) = \frac{\varepsilon_w}{2-\varepsilon_w}(\theta_2 - \theta_1). \tag{46}$$

The P_1-approximation prediction, equation (45), results in

$$\lim_{\tau_0\to 0} Q(0) = \frac{2\varepsilon_w}{3k+2(1-\varepsilon_w)}(\theta_2 - \theta_1). \tag{47}$$

Equation (47) shows that the heat transfer rate to Wall 1 predicted by the P_1-approximation in the limit of $\tau_0 \to 0$ is not equal to the exact solution unless k takes the value of 2/3, i.e. n is equal to 1 as $k = n + 1/n + 2$ or the two walls are at the same temperature, i.e. $\theta_1 = \theta_2$.

In the case that τ_0 tends to infinity, the exact heat transfer rate to Wall 1 is given as

$$\lim_{\tau_0\to\infty} Q_e(0) = \varepsilon_w(1-\theta_1). \tag{48}$$

The P_1-approximation, however, yields

$$\lim_{\tau_0\to\infty} Q(0) = \frac{4\frac{\sqrt{3}}{3}}{1+\frac{\sqrt{3}}{3}\frac{3k+2(1-\varepsilon_w)}{\varepsilon_w}}(1-\theta_1). \tag{49}$$

Comparison of equation (49) with equation (48) indicates that the P_1-approximation prediction of the heat transfer rate to Wall 1 in the optically thick limit is not accurate unless k takes the following value:

$$k = \frac{2}{3} + \left(\frac{2}{3} - \frac{\sqrt{3}}{3}\right)\varepsilon_w. \tag{50}$$

It is worth noting that this 'optimum' k is dependent on the wall emissivity ε_w. Correspondingly, the value of n can be estimated from equation (50) for a given wall emissivity using the relation of equation (24). As the value of the wall emissivity ε_w is between 0 and 1, equation (50) reveals that the 'optimum' k satisfies

$$0.6667 \leqslant k \leqslant 0.7560. \tag{51}$$

The corresponding value of n is either 1 or 2, depending on the wall emissivity ε_w. If ε_w is smaller than 0.5, it is recommended to use $n = 1$; however, if ε_w is greater than 0.5, it is preferable to use $n = 2$. These suggestions will be validated and complemented by comparing the P_1-approximation results of the heat transfer rate to Wall 1 with the exact solution for different wall emissivities numerically.

Numerical results of non-dimensional heat transfer rate to Wall 1, $Q(0)$, are plotted in Fig. 2 as a function of optical dimension τ_0. It can be seen from Fig. 2 that when n is not equal to 1 the P_1-approximation does not predict the correct heat transfer rate to Wall 1 in the optically thin limit as indicated by equations (46) and (47). The results show that this discrepancy decreases with decreasing wall emissivity. The P_1-approximation results in the limit of $\tau_0 \to 0$ are independent of n if θ_1 is equal to θ_2 (see equation (47)). It is clearly shown in Fig. 2 that the influence of n on the P_1-approximation results is indeed dependent on the wall emissivity ε_w. For high wall emissivities, $\varepsilon_w > 0.5$, the use of $n = 2$ yields a much more accurate heat transfer rate to Wall 1 than the use of $n = 1$ (see (a) and (b)). For intermediate wall emissivities, when

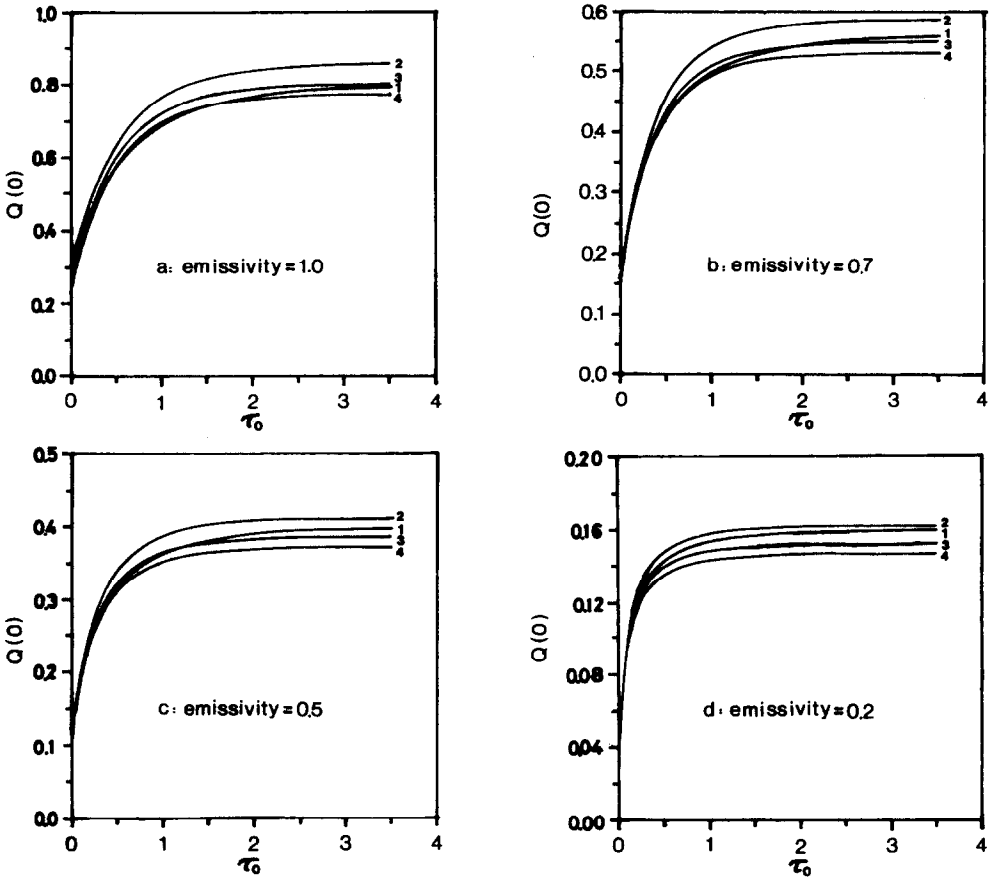

FIG. 2. Comparisons of non-dimensional heat transfer rates to Wall 1 obtained by the P_1-approximation using different boundary conditions with exact solutions for different wall emissivities: $\theta_1 = 0.2$, $\theta_2 = 0.5$. (1) Exact solution; (2) P_1, $n = 1$; (3) P_1, $n = 2$; (4) P_1, $n = 3$.

$\varepsilon_w \approx 0.5$, then the use of $n = 2$ is still superior to that of $n = 1$, especially at small and intermediate optical dimensions (see (c)). For low wall emissivities, when $\varepsilon_w < 0.5$, then it is preferable to use $n = 1$, i.e. Marshak's boundary condition (see (d)). Another suggestion which may be inferred from Fig. 2 is that for very high wall emissivities, $\varepsilon_w \geqslant 0.7$, it is better to use $n = 3$ rather than $n = 2$ at intermediate optical dimensions (see (a) and (b)). It should be pointed out that the influence of n on the P_1-approximation results becomes more pronounced as the optical dimension increases.

3.2. *Two-dimensional problems*

For two-dimensional radiative heat transfer problems, two cases with different thermal conditions are considered in Cartesian coordinates.

Firstly, consider an infinitely long square cavity containing a medium of uniform temperature and uniform absorption coefficient where all four wall surfaces are cold and black. Exact solutions for surface heat transfer rates are available due to Lockwood and Shah [12]. The P_1-approximation results for non-dimensional surface heat transfer rates are compared with exact solutions in Figs. 3–5. In obtaining the results of the P_1-approximation numerically, various grid schemes were tested, and it was found that the results obtained using a finer grid differed relatively little from the results using a coarser grid for small and intermediate optical dimensions. However, this difference became greater as the optical dimension increased. All the numerical results of the P_1-approximation reported for this problem were obtained using a 20×20 uniform grid scheme. It was also found that the computing time depends strongly on the optical dimension. The CPU times required were 1, 5 and 13 s when the optical dimensions of the cavity were 10, 1.0 and 0.1, respectively.

Figures 3–5 show the surface heat transfer rates of the P_1-approximation using different boundary conditions for different optical dimensions. In these figures, $n = 1$ represents Marshak's boundary condition. Different values of n, such as 0, 2, 3 and 4, have been used to calculate the P_1-approximation results. It was found that $n = 3$ is the optimum boundary condition. It is clear that the P_1-approximation using Marshak's boundary condition of $n = 1$ overpredicts the surface heat flux, especially for the large optical dimension $\tau_0 = 10$, where the P_1-approximation yields unrealistic values of heat flux (greater than unity). How-

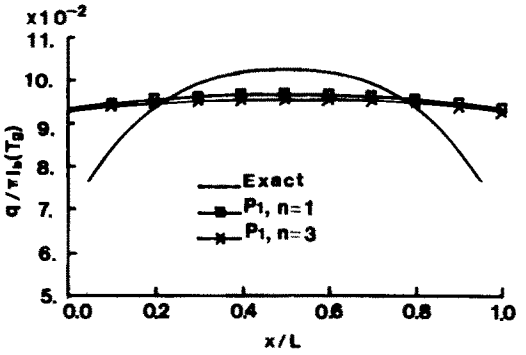

FIG. 3. Influence of the boundary condition on the prediction of the P_1-approximation for the non-dimensional surface heat transfer rate: $\tau_0 = 0.1$.

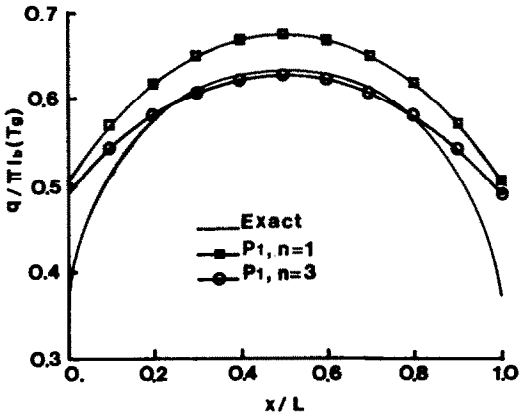

FIG. 4. Influence of the boundary condition on the prediction of the P_1-approximation for the non-dimensional surface heat transfer rate: $\tau_0 = 1.0$.

ever, if $n = 3$ is employed, the surface heat transfer rates are improved significantly except for the optically thin case where it is believed that the differential approximation loses its validity. In the optically thin case (Fig. 3), the P_1-approximation cannot predict the correct variation trend of the heat flux distribution. In addition, the boundary conditions have only a slight influence on the solution. For intermediate optical dimensions (Fig. 4), the P_1-approximation using the boundary condition of $n = 3$ predicts accurate surface heat flux in the region removed from the corner region; however, it still overpredicts the heat flux in the corner region. For the case of large optical dimension (Fig. 5), the P_1-approximation when using $n = 3$ yields very accurate surface heat transfer rates, even near the corner. Based on these findings, it can be concluded that the boundary condition with $n = 3$ is superior to Marshak's boundary condition. However, it is worth noting that the results of the P_1-approximation for small and intermediate optical dimensions cannot be further improved, due to the nature of the differential approximation, by selecting different values of n. However, the influence of n on the P_1-approximation increases with increasing optical dimension, which has been observed in Fig. 2.

The second case has the same geometry as the last one but has different thermal conditions. In this case, the bottom wall is at a dimensionless temperature of unity. The other three walls are cold. All the walls are black and the medium is subject to a uniform heat generation of zero, i.e. the medium is in radiative equilibrium. The optical dimension of this cavity is unity. For this problem, numerical results of the zone method have been presented [7]. The results of the P_1-approximation using different boundary conditions are compared with the zone method results in Figs. 6

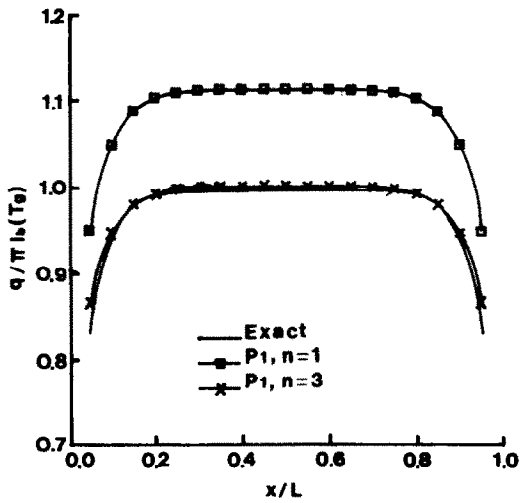

FIG. 5. Influence of the boundary condition on the prediction of the P_1-approximation for the non-dimensional surface heat transfer rate: $\tau_0 = 10$.

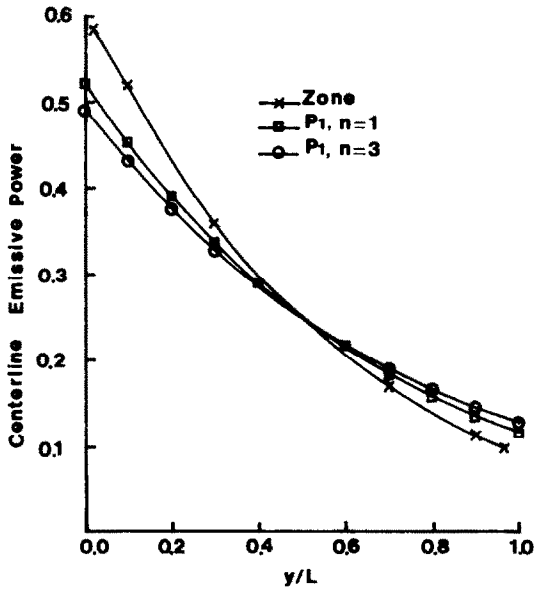

FIG. 6. Influence of the boundary condition on the prediction of the P_1-approximation for the non-dimensional centreline emissive power distribution: $\tau_0 = 1.0$.

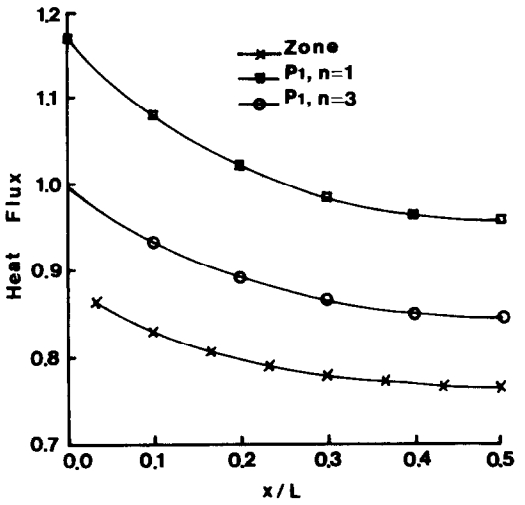

FIG. 7. Influence of the boundary condition on the prediction of the P_1-approximation for the non-dimensional hot surface heat transfer rate: $\tau_0 = 1.0$.

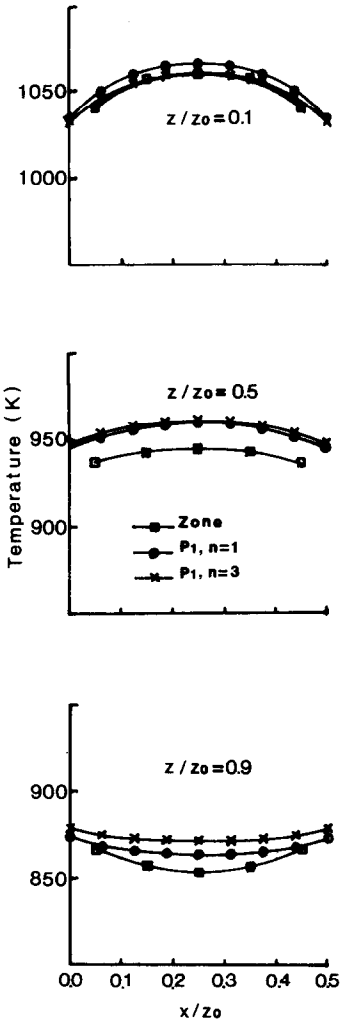

FIG. 8. Influence of the boundary condition on the prediction of the P_1-approximation for temperature distributions at three axial locations: $\kappa_x = 1.0\ \mathrm{m}^{-1}$, $y/z_0 = 0.25$.

and 7. Numerical results of the P_1-approximation were obtained using a 10×10 uniform grid scheme. Figure 6 shows the non-dimensional centreline emissive power distribution. The P_1-approximation underestimates the emissive power near the hot surface and overestimates the power near the cold surface. Note that the use of the boundary condition $n = 3$ yields a slightly worse centreline emissive power distribution than the use of Marshak's boundary condition. Figure 7 shows the non-dimensional heat transfer rate for the hot surface. It is clearly shown that the boundary condition of $n = 3$ is much better than Marshak's boundary condition. Although the heat transfer rate for the hot surface can be further improved by using a greater n, it will give rise to further deterioration of the centreline emissive power distribution.

3.3. *Three-dimensional problems*

Consider a radiative transfer problem in an idealized furnace subject to uniform heat generation. The data assumed in the predictions are given in Table 1.

For this problem, the zone method results of Menguc and Viskanta [2] are used as exact solutions to study the influence of n on the P_1-approximation. In performing the numerical calculations, the medium was divided into $8 \times 8 \times 10$ uniform control volumes. The computing time required by the P_1-approximation was only 7 s. Numerical calculations were performed for the furnace having an optical dimension ($\kappa_x z_0$) of 1.0. The temperature distributions obtained by the P_1-approximation at three axial locations of the furnace are compared with the predictions based on the zone method in Fig. 8. Near the hot wall ($z/z_0 = 0.1$), the P_1-approximation predicts accurate temperature distributions. At the centre of the furnace ($z/z_0 = 0.5$) and near the cold end wall ($z/z_0 = 0.9$), the P_1-approximation overpredicts the medium temperatures by as much as 5%. It is worth noting that predictions of temperature distributions using different boundary conditions differ only slightly from each other, especially at the centre of the furnace.

Table 1. Physical parameters of the idealized furnace

Medium	$S = 5.0\ \mathrm{kW\,m^{-3}}$ $x_0 = 2\,\mathrm{m}$, $y_0 = 2\,\mathrm{m}$, $z_0 = 4\,\mathrm{m}$
Boundaries	$z = 0$, $T = 1200\,\mathrm{K}$, $\varepsilon_w = 0.85$ $z = z_0$, $T = 400\,\mathrm{K}$, $\varepsilon_w = 0.7$ others, $T = 900\,\mathrm{K}$, $\varepsilon_w = 0.7$

The radiative heat fluxes at the hot and the cold end walls are compared in Fig. 9 with those obtained from the zone method. The P_1-approximation, when using Marshak's boundary condition, overpredicts the heat transfer rate at the hot end wall by as much as 15%; however, this difference decreases to under 5% when the boundary condition of $n = 3$ is used. It should be pointed out that for this problem the P_1-approximation,

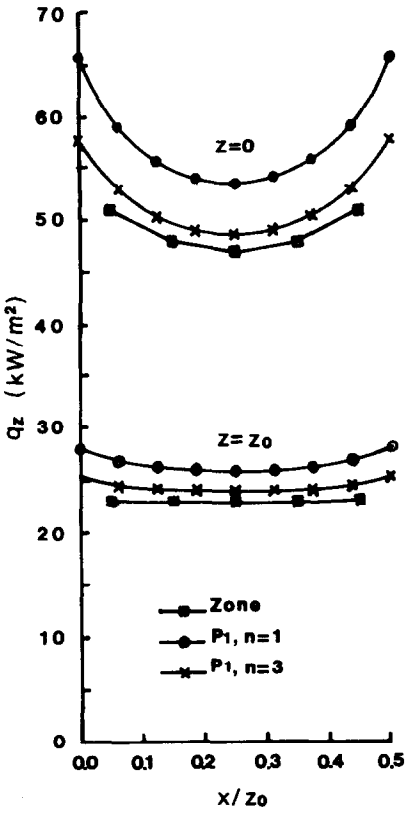

FIG. 9. Influence of the boundary condition on the prediction of the P_1-approximation for surface heat transfer rate at two end walls: $\kappa_x = 1.0\ m^{-1}$, $y/z_0 = 0.25$.

when using the boundary condition of $n = 3$, predicts the surface heat fluxes as accurately as the P_3-approximation of Menguc and Viskanta [2], although their results are not plotted in the figure. However, the temperature predictions of the P_1-approximation are slightly less accurate than the P_3-approximation.

4. CONCLUSIONS

The influence of boundary condition on the predictions of the P_1-approximation has been investigated for both one- and multi-dimensional radiative heat transfer problems. It is found that the accuracy of the P_1-approximation can be improved significantly if the optimized value of n is used in the boundary condition. The effect of n on the results of the P_1-approximation becomes more pronounced as the optical dimension of the radiating system considered increases. Although the P_1-approximation using the boundary condition of $n = 3$ sometimes yields slightly worse results for the medium emissive power or temperature distributions for problems with specified volumetric heat generation, it predicts the radiative heat flux at boundaries much more accurately. Moreover, the prediction of emissive power is much less sensitive to the boundary condition than the surface heat flux.

Based on the numerical studies performed in this work, some recommendations for the choice of the value of n can be made. For one-dimensional problems, it is suggested that $n = 2$ be used if the wall emissivity of the system is high or intermediate; however, $n = 1$ or Marshak's boundary condition should be employed for the P_1-approximation if the wall emissivity is low. For multi-dimensional problems, the P_1-approximation when using $n = 3$ as the boundary condition predicts much more accurate surface heat transfer rates than the use of $n = 1$. It should be noted that this recommendation for multi-dimensional problems is applicable for high wall emissivities. No assessment has been made in this work for low wall emissivities since exact solutions for such cases do not exist in the literature. However, most wall surfaces encountered in practical combustion systems have emissivities of about 0.7 or higher.

Since the simple P_1-approximation offers the advantages of high computational efficiency and compatibility with the finite difference technique frequently used in computational fluid dynamics, together with the improved accuracy demonstrated in this work, it is attractive for use in general prediction procedures.

Acknowledgements—This work was jointly supported by the British Council and the Chinese government.

REFERENCES

1. R. Viskanta and M. P. Menguc, Radiative heat transfer in combustion systems, *Prog. Energy Combust. Sci.* **13,** 97–160 (1987).
2. M. P. Menguc and R. Viskanta, Radiative transfer in three-dimensional rectangular geometries containing inhomogeneous, anisotropic scattering media, *J. Quant. Spectrosc. Radiat. Transfer* **33,** 533–549 (1985).
3. M. P. Menguc and R. Viskanta, Radiative transfer in axisymmetric, finite cylindrical enclosures, *J. Heat Transfer* **108,** 271–276 (1986).
4. B. Davison, *Neutron Transport Theory*, Section 10.3. Clarendon Press, Oxford (1958).
5. G. C. Pomraning and G. M. Foglesong, Transport–diffusion interfaces in radiative transfer, *J. Comput. Phys.* **32,** 420–436 (1979).
6. K. M. Case and P. F. Zweifel, *Linear Transport Theory*, p. 212. Addison-Wesley, Reading, MA (1967).
7. A. C. Ratzel and J. R. Howell, Two-dimensional radiation in absorbing–emitting media using the *P–N* approximation, *J. Heat Transfer* **105,** 333–340 (1983).
8. F. Liu, New development in pulverised coal combustion: numerical modelling of radiative heat transfer and experimental test of a novel burner technique, Ph.D. Thesis, Department of Mechanical and Process Engineering, University of Sheffield, Sheffield, U.K., p. 145 (1990).
9. J. Higenyi and Y. Bayazitoglu, Differential approximation of radiative heat transfer in a grey medium, *J. Heat Transfer* **102,** 719–723 (1980).
10. T. J. Love, *Radiative Heat Transfer*, p. 118. Charles E. Merrill, Columbus, OH (1968).
11. R. Siegel and J. R. Howell, *Thermal Radiation Heat Transfer*, 2nd Edn, p. 842. McGraw-Hill, New York (1981).
12. F. C. Lockwood and N. G. Shah, A new radiation solution method for incorporation in general combustion prediction procedures, *18th Symp. (Int.) on Combustion*, The Combustion Institute, pp. 1405–1414 (1981).

SUR LA CONDITION LIMITE DE L'APPROXIMATION P_N UTILISEE POUR RESOUDRE L'EQUATION DE TRANSFERT RADIATIF

Résumé—L'arbitraire de la condition limite appliquée à l'approximation P_1 est exploré en étendant la condition limite conventionnelle de Marshak pour inclure une constante arbitraire. L'influence de la constante sur les résultats de cette approximation est étudiée numériquement pour des problèmes de transfert radiatif à une ou plusieurs dimensions. A partir de cette étude, on recommande des valeurs optimales de la constante en tenant compte de l'émissivité des parois. La précision de l'approximation peut être augmentée sensiblement quand des valeurs optimisées sont employées dans la condition limite.

DIE RANDBEDINGUNG BEI DER P_N-APPROXIMATION ZUR LÖSUNG DER GLEICHUNG FÜR STRAHLUNGSTRANSPORT

Zusammenfassung—Die Freiheit bei der Wahl der Randbedingung bei der P_1-Approximation wird erforscht, indem die konventionelle Marshak-Randbedingung um eine beliebige Konstante erweitert wird. Der Einfluß der Konstanten auf die Ergebnisse der P_1-Approximation wird numerisch für ein- und mehrdimensionale Probleme des Strahlungswärmetransports untersucht. Auf der Grundlage dieser numerischen Untersuchungen werden Optimalwerte für die Konstante empfohlen entsprechend dem Emissionsvermögen der Wand des strahlenden Systems. Die Genauigkeit der P_1-Approximation kann signifikant durch Anwendung optimierter Werte in der Randbedingung verbessert werden.

ГРАНИЧНОЕ УСЛОВИЕ P_N-АППРОКСИМАЦИИ, ИСПОЛЬЗУЕМОЕ ДЛЯ РЕШЕНИЯ УРАВНЕНИЯ РАДИАЦИОННОГО ПЕРЕНОСА

Аннотация—Посредством введения произвольной постоянной в общепринятое граничное условие Маршака исследуются варианты граничного условия, используемого в P_1-аппроксимации. Численно определяется влияние этой постоянной на результаты P_1-аппороксимации для одно- и многомерных задач радиационного теплопереноса. На основе численных исследованний рекомендуются оптимизированные значения постоянной, соответствующие эмиссионной способности стенки излучающей системы. Точность P_1-аппорогсимации может быть существенно повышена при использовании оптимизированных значений в граничном условии.